CHAPTER 3

RESULTS

3.1 Production Yield of Gelatin Extraction, Gelatin Hydrolysate Preparation and Their Degree of Hydrolysis (DH)

Frozen Nile tilapia skins were defrosted and clean up with tap water to remove scale that still attached to the skin, followed by cutting it into small square pieces. After that, noncollagenous proteins and pigments on the skins were removed by alkaline treatment for 2 hrs. The alkaline treated skin was washed up with tap water for 1 hr and additionally treated with HCl for 1 hr. The acid was used to unwind the triple helix structure of collagen for better gelatin extraction. Tap water was used to wash the resulted transparent skin until the neutral pH of washing water was obtained. Gelatin was extracted by heating with water to 60 °C and the solution was filtered through double layer cheesecloth. The solution was, then, lyophilized and weighed. The average production yield of tilapia skin gelatin was 20.77 ± 0.80% wet weight basis (Table 3.1).

Table 3.1 Production yield of gelatin from Nile tilapia skin

Extraction	Wet fish skin (g)	Lyophilized gelatin (g)	Yield (%)
1	33.43	6.64	19.86
2	30.28	6.45	21.30
3	30.01	6.35	21.16

To prepare gelatin hydrolysate, bromelain, papain, trypsin, alcalase, flavourzyme and neutrase were applied to gelatin and hydrolyze with their reported optimal conditions for 4 hrs. The hydrolysate mixture was investigated for DH by react with TNBS solution. The primary amino group (α-amino acid) formed the orange colored product with TNBS which absorbs maximally at 420 nm. The %DH of each hydrolysate was presented in Figure 3.1.

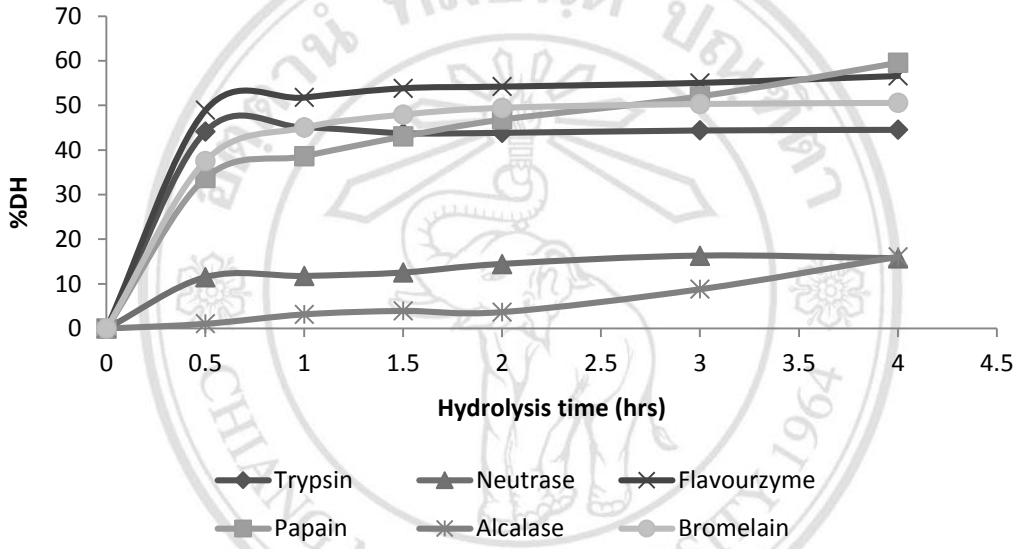

Figure 3.1 Degree of hydrolysis percentage of each hydrolysate

Within 4 hrs of hydrolysis, it was noticed that three hydolysates had reached DH higher than 50%, which were papain (59.55 ± 0.014%), flavourzyme (56.61 ± 0.011%) and bromelain (50.59 ± 0.024%). The DH of trypsin hydrolysate was lower than those hydrolysates (44.55 ± 0.010%). Among all hydrolysates, alcalase and neutrase showed the lowest DH of 16.05 ± 0.014% and 15.71 ± 0.016%, respectively. Interestingly, flavourzyme, bromelain, neutrase and trypsin reached their maximum DH approximately in 1.5 hrs, while, the DH from papain and alcalase increased continuously during the entire experiment.

3.2 Bioactivities of Nile Tilapia Gelatin Hydrolysate

Nile tilapia gelatin hydrolysate that was obtained from different enzymatic hydrolysis was fractionated by Amicon® Ultra-15 centrifugal filter devices with MWCO 10,000 Da. Two fractions, filtrates (MW<10 kDa) and retentate (MW>10 kDa), of each hydrolysate were quantified for antioxidant and antihypertensive activities. However, the retentate fractions of all hydrolysate did not exhibit both antioxidant and antihypertensive activities. So, only the filtrate was reported and discussed afterward in this thesis. The protein concentration of filtrates was determined by Bradford method (see Appendix B-1). The protein contents in the filtrates of bromelain, flavourzyme, trypsin, alcalase, papain and neutrase were 0.067, 0.053, 0.060, 0.048, 0.072 and 0.070 mg/mL, respectively.

3.2.1 Determination of Antioxidant Activities

Four methods, which were ABTS radical scavenging assay, FRAP assay, ferrous ion chelating assay and lipid peroxidation inhibition assay, were applied to determine the level of antioxidant properties of the gelatin hydrolysate. Based on their oxidizing reagents, it can be classified into two groups: metal ions (FRAP and ferrous ion chelating) and organic radicals (ABTS and lipid peroxidation inhibition). The reaction mechanism of lipid peroxidation assay, though, differs from the other three methods. For lipid peroxidation inhibition assay, the delay of radical generation along with the radical scavenging ability is evaluated. While, the reducing ability of the test sample on radical cations or metal ion is analyzed in the other three assays.

1) ABTS Radical Scavenging Activity

This assay based on the ability of antioxidants to scavenge the $ABTS^{+\bullet}$ radical. Peroxyl radicals or other oxidants are used to oxidize ABTS to its intensively colored radical cation, $ABTS^{+\bullet}$. The antioxidant capacity is measured as the ability of test compounds to reduce the $ABTS^{+\bullet}$ radical, concomitantly decreasing the intense green color. The results are calculated relatively to Trolox standard curve (see Appendix B-2) and expressed as μg trolox/mg protein. The results were presented in the Table 3.2.

Flavourzyme and trypsin hydrolysate exhibited the highest ABTS activity with 282.65 ± 17.74 and 263.21 ± 8.78 mM trolox/mg protein, respectively. The lowest activity occurred in papain and neutrase hydrolysate. Interestingly, alcalase hydrolysate did not exhibit any ABTS activity within 10 min of reaction.

2) FRAP Assay

FRAP method uses the yellow iron complex, ferric tripyridyl triazine (Fe^{3+}-TPTZ), as a testing reagent. After reacting with antioxidants, Fe^{3+}-TPTZ is reduced and the blue complex of Fe^{2+}-TPTZ took place. The results was calculated and reported as trolox equivalent (mM trolox/mg protein) from the trolox standard curve (see Appendix B-3). FRAP results were showed in the Table 3.2.

All hydrolysate could reduce the iron complex into the intense blue complex of Fe^{2+}-TPTZ, ranging from 2.84-4.95 mM trolox/mg protein. Alcalase hydrolysate was found to possess the highest reducing power, while, the lowest was noticed in bromelain hydrolysate.

3) Chelating Activity on Ferrous Ion

Iron is an important ion that involves with Fenton reaction to generate the free radicals. So, chelating of free Fe^{2+} is one way to prevent or diminish the generated free radicals. This assay determined the ability of active peptide in gelatin hydrolysate to chelate Fe^{2+}. Free Fe^{2+} reacts with ferrozine and becomes the purple Fe^{2+}-ferrozine complex. The more Fe^{2+} to respond with, the more intense purple color observed. The chelating activity of each hydrolysate was exhibited in Table 3.2.

It was found out that most gelatin hydrolysates had the great ability to trap the Fe^{2+}. The great chelating activity of Fe^{2+} was manifested with the chelation percentage higher than 75%, except for papain hydrolysate, of which only 15.78 ± 0.02% of was noticed.

4) Inhibitory Activity on Lipid Peroxidation in Linoleic Acid Model

The inhibition of lipid peroxidation is based on the ability of test sample to inhibit or delay lipid autooxidation. In linoleic acid model system, lipid peroxyl radical, primary oxidized lipid products, further oxidizes ferrous ion to generate ferric ion. Produced ferric ions react

with ammonium thiocyanate to form the ferric thiocyanate complex, resulting in red color development. The color intensity is proportional to the concentration of oxidized lipid.

In Table 3.2, the results displayed that over 50% of inhibition were discoverd in three hydrolysate, which were flavourzyme (59.74 ± 16.57%), trypsin (56.71 ± 7.16%) and bromelain (56.61 ± 13.26%), and were not significantly different (p>0.05) from the positive control, 4 mM trolox (70.27 ± 7.27%). Papain hydrolysate could inhibit the oxidation of lipid with 41.56 ± 1.22%. While, low level of inhibition (approximately 30%) was observed in alcalase and neutrase hydrolysate.

Non-hydrolyzed Nile tilapia gelatin exhibited low potency as antioxidant agent. In ABTS radical scavenging assay, only 8.83 ± 2.57 µg trolox/mg protein was noticed from non-hydrolyzed gelatin. For FRAP assay, non-hydrolyzed gelatin was negligible in reducing the Fe^{3+}-TPTZ complex. Very low ferric chelating percentage (8.34 ± 0.68%) and inhibition percentage of lipid oxidation (7.90 ± 1.10%) were also noticed. From these results, it could be concluded that peptide hydrolysates produced by different enzymes showed distinct levels of antioxidant activity. These different levels of antioxidant activity may contribute to different fragmented peptides in the hydrolysates.

Table 3.2 Antioxidative properties of Nile tilapia gelatin hydrolysate with MW<10 kDa from different enzyme

Hydrolysate	ABTS (mM trolox/mg protein)	FRAP (mM trolox/mg protein)	Ferrous ion chelating (%chelating activity)	Lipid peroxidation (%inhibition)
Non-hydrolyzed	1.77 ± 0.51^{a}	0.01 ± 0.00^{a}	8.34 ± 0.68^{a}	7.90 ± 1.10^{a}
Bromelain	214.41 ± 5.91^{b}	2.84 ± 0.48^{b}	86.90 ± 0.06^{d}	56.61 ± 13.26^{c}
Papain	51.19 ± 24.37^{c}	$3.48 \pm 0.19^{b,c}$	15.78 ± 0.02^{b}	$41.56 \pm 1.22^{b,c}$
Trypsin	263.21 ± 8.78^{d}	$3.47 \pm 0.47^{b,c}$	$83.61 \pm 0.04^{c,d}$	56.71 ± 7.16^{c}
Alcalase	ND	4.95 ± 0.33^{d}	77.28 ± 0.05^{c}	$29.22 \pm 8.26^{a,b}$
Flavourzyme	282.65 ± 17.74^{d}	$4.27 \pm 1.16^{c,d}$	85.09 ± 0.12^{d}	59.74 ± 16.57^{c}
Neutrase	37.30 ± 3.47^{c}	$4.15 \pm 0.16^{c,d}$	$83.43 \pm 0.01^{c,d}$	$29.01 \pm 14.08^{a,b}$

ND: not detectable

Different letters represent significant differences (p<0.05).

3.2.2 Evaluation of ACE Inhibitory Activity

ACE is a major factor in regulating blood pressure in RAS. It turns angiotensin I, an inactive form, into angiotensin II, a potent vasoconstrictor, and inhibits bradykinin activity, which involved in lowering blood pressure. This assay evaluated the inhibitory activity of test sample against ACE action and used HHL as a substrate. HHL was converted to hippuric acid, which detected by UV spectrometer. Each gelatin hydrolysate was tested for their ACE inhibitory activity and the results were displayed in Figure 3.2.

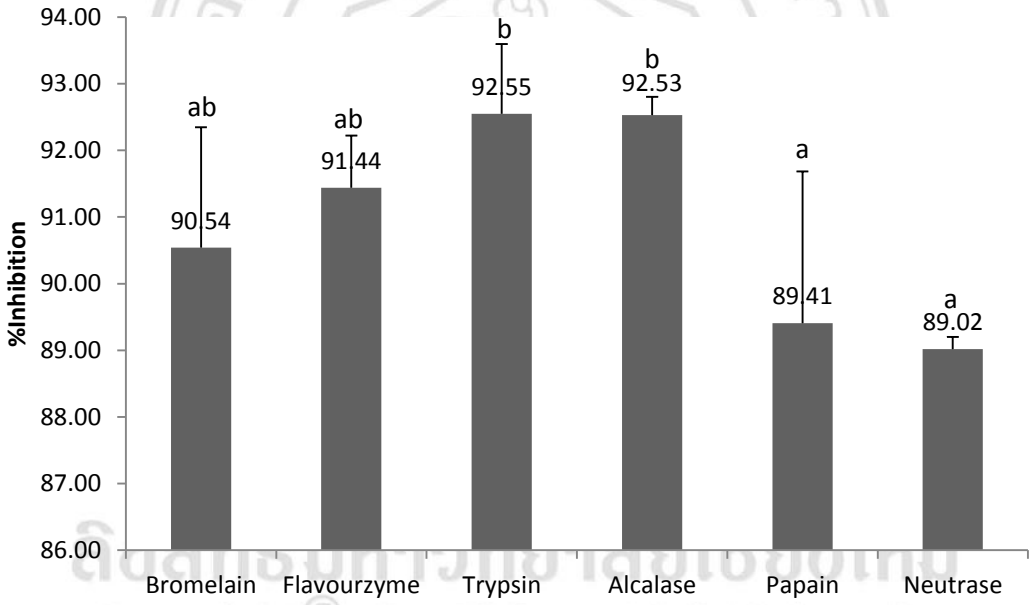

Figure 3.2 Inhibition percentage of ACE with different Nile tipalia skin gelatin hydrolysate. Different alphabets indicate significant differences (p<0.05).

It was found that all hydrolysates showed great potential as ACE inhibitory agent. The percentage inhibition ranged from 89.02-92.55%. The best inhibition was noticed in trypsin and alcalase hydrolysate. The lowest activity found in papain and neutrase hydrolysate, but still presented nearly 90% inhibition. Non hydrolyzed gelatin could not inhibit the activity of ACE.

After evaluation of bioactivities of gelatin hydrolysate with MW lower than 10 kDa, two hydrolysates that possessed the best bioactivities were selected for further purification to obtain purified peptide. Among these, flavourzyme hydrolysate was found to be the best bioactive hydrolysate since it exhibited higher level of antioxidant activity in every assay. It also greatly inhibited the ACE activity. Papain and neutrase were cut off from further purification because their antihypertensive activity was not the highest and did not showed great antioxidant activity. For papain hydrolysate, it had poor ferrous chelating activity and could reduce $ABTS^{\cdot}$ in low level. Neutrase had same level as papain in term of the ability for reducing $ABTS^{\cdot}$. Furthermore, neutrase could not prevent the oxidation of lipid as well. Alcalase hydrolysate had displayed an excellent activity in FRAP and ACE inhibition assay and also had great chelating activity too. However, without detectable capacity in ABTS method and low potency in prevention of lipid oxidation, alcalase was not the suitable sample for further experiment. Bromelain hydrolysate exhibited high level of antioxidant activities similar to trypsin hydrolysate, nevertheless, the inhibition of ACE activity of bromelain was slightly lower than trypsin. Therefore, trypsin hydrolysate, the hydrolysate that possessed high potential as both antioxidant and antihypertensive agents, was selected for further purification and sequence identification together with flavourzyme hydrolysate.

3.3 Purification of Bioactive Peptide Using Gel Filtration Chromatography and Ion Exchange Chromatography

First, the peptides in hydrolysate were fractionated according to their molecular weights. DI ultra-pure water used to dissolve lyophilized crude trypsin and flavourzyme hydrolysates and the hydrolysate solutions were separately applied to Sephadex® G-50

gel filtration column. DI water was used as an eluent with a flow rate of 1 mL/min. Three significant peaks were obtained from trypsin hydrolysate, which were tagged as TA (tube 18-28), TB (tube 45-60) and TC (tube 63-68) (Figure 3.3A). While, flavourzyme hydrolysate gave 4 fractions, labelled as FA (tube 19-31), FB (tube 32-48), FC (tube 49-59) and FD (tube 60-74) (Figure 3.3B). Production yield for each fraction was 1.89 ± 0.02% (TA), 38.97 ± 0.04% (TB), 34.18 ± 0.04% (TC), 1.17 ± 0.01% (FA), 18.62 ± 0.01% (FB), 19.71 ± 0.04% (FC) and 37.71 ± 0.04% (FD). These obtained fractions were quantified for antioxidant activity with ABTS assay and antihypertensive activity. The results were shown in Table 3.3. Among all sample, the highest antioxidant activity was noticed in FA fraction with 280.45 ± 0.61 mM trolox/mg protein, followed by FD fraction with 250.05 ± 0.02 mM trolox/mg protein. Interestingly, both crude trypsin and crude flavourzyme could exhibit great antioxidant properties (205.80 ± 0.29 and 235.65 ± 0.34, respectively). The antioxidant activity of fractionates from trypsin hydrolysate (TA, TB and TC) had lower than the activity of the crude trypsin hydrolysate the same as FB and FC fraction compared to crude flavourzyme hydrolysate.

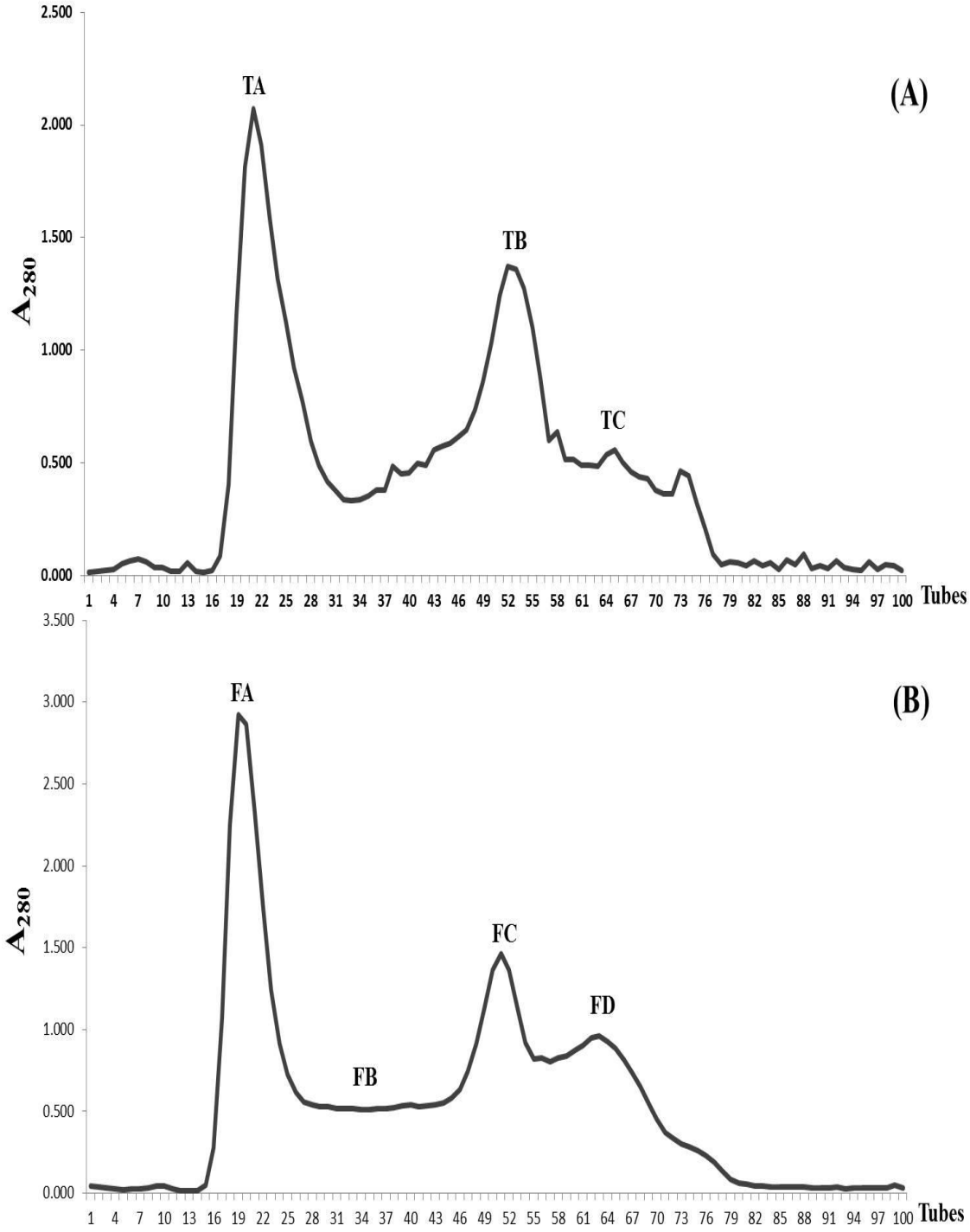

Figure 3.3 Chromatogram of gelatin hydrolysate from Nile tilapia skin fractionated by Sephadex® G-50 column that was eluted with DI water at flow rate of 1 mL/min. (A): Trypsin hydrolysate and (B): Flavourzyme hydrolysate

Table 3.3 The bioactivity of fractionated peptides from trypsin and flavourzyme hydrolysate by Sephadex® G-50 column

Sample	ABTS (mM trolox/mg protein)	ACE inhibition (%)
Crude Trypsin	$205.80 \pm 0.29^{a,b,c}$	56.22 ± 2.19^{a}
TA	116.15 ± 0.70^{b}	28.80 ± 9.11^{b}
TB	$163.15 \pm 0.44^{a,b}$	$59.33 \pm 9.97^{a,c}$
TC	$186.80 \pm 0.38^{a,b,c}$	40.59 ± 5.89^{b}
Crude Flavourzyme	$235.65 \pm 0.34^{a,c}$	83.60 ± 0.98^{d}
FA	280.45 ± 0.61^{c}	$73.69 \pm 6.83^{c,d}$
FB	113.95 ± 0.10^{b}	82.40 ± 2.72^{d}
FC	$164.90 \pm 0.13^{a,b}$	$68.28 \pm 1.26^{a,c}$
FD	$250.05 \pm 0.02^{a,c}$	79.53 ± 2.00^{d}

Different letters represent significant differences (p<0.05).

For antihypertensive activity, the superior inhibition was observed from all flavourzyme fractions, ranging from 68-83 inhibition percentages. While, in trypsin fraction, only crude and TB fraction could inhibit ACE activity higher than 50%. TA and TC fraction was not good for inhibition of ACE with percentage of inhibition lower as 28.80 ± 9.11 and 40.59 ± 5.89, respectively. One of the best fractions of each enzyme hydrolysate was selected for further purification by ion exchange chromatography by compared with antioxidant and antihypertensive activity together with their production yield. For trypsin, TB and TC fraction showed the same level of production yield (38.97 ± 0.04 and 34.18 ± 0.04%, respectively) and antioxidant activity (163.15 ± 0.44 and 186.80 ± 0.38 mM trolox/mg protein, respectively), nevertheless, TB fraction had greater activity in ACE inhibition than TC fraction significantly. In case of flavourzyme, even if, FA fraction possessed great potency for both antioxidant and antihypertensive activity but, with their slight yield, this fraction may be not the best fraction for further development. FB fraction demonstrated the greatest inhibitory activity against ACE (82.40 ± 2.72%) but it lacked ability as antioxidantive agent (113.95 ± 0.10 mM trolox/mg protein). By comparing FC fraction with FD fraction, that FD fraction showed better performance than FC fraction in every aspectss; more production yield (37.71 ± 0.04 to 19.71 ± 0.04%), higher antioxidant activity (250.05 ± 0.02 to 164.90 ± 0.13 mM trolox/mg protein) and greater inhibition for ACE (79.53 ± 2.00 to 68.28 ± 1.26). So, TB and FD fraction were further purified with SP sephadex® C-25 ion exchange chromatography. Sodium acetate buffer (20 mM, pH 4.0) was used to elute peptide from the column with linear gradient of NaCl (0-1.0 M) at flow rate 0.6 mL/min. One single peak (TB1; tube 7-10) was observed from TB fraction and two peaks were obtained from FD fraction, designated as FD1 (tube 9-12) and FD2 (tube

13-16), respectively (Figure 3.4). Nevertheless, FD1 and FD2 fractions did not completely separated from each other. Collected fractions were examined for their bioactivities again to search for the preferable fraction for peptide sequence analysis. Table 3.4 demonstrated the bioactivity results of each fraction.

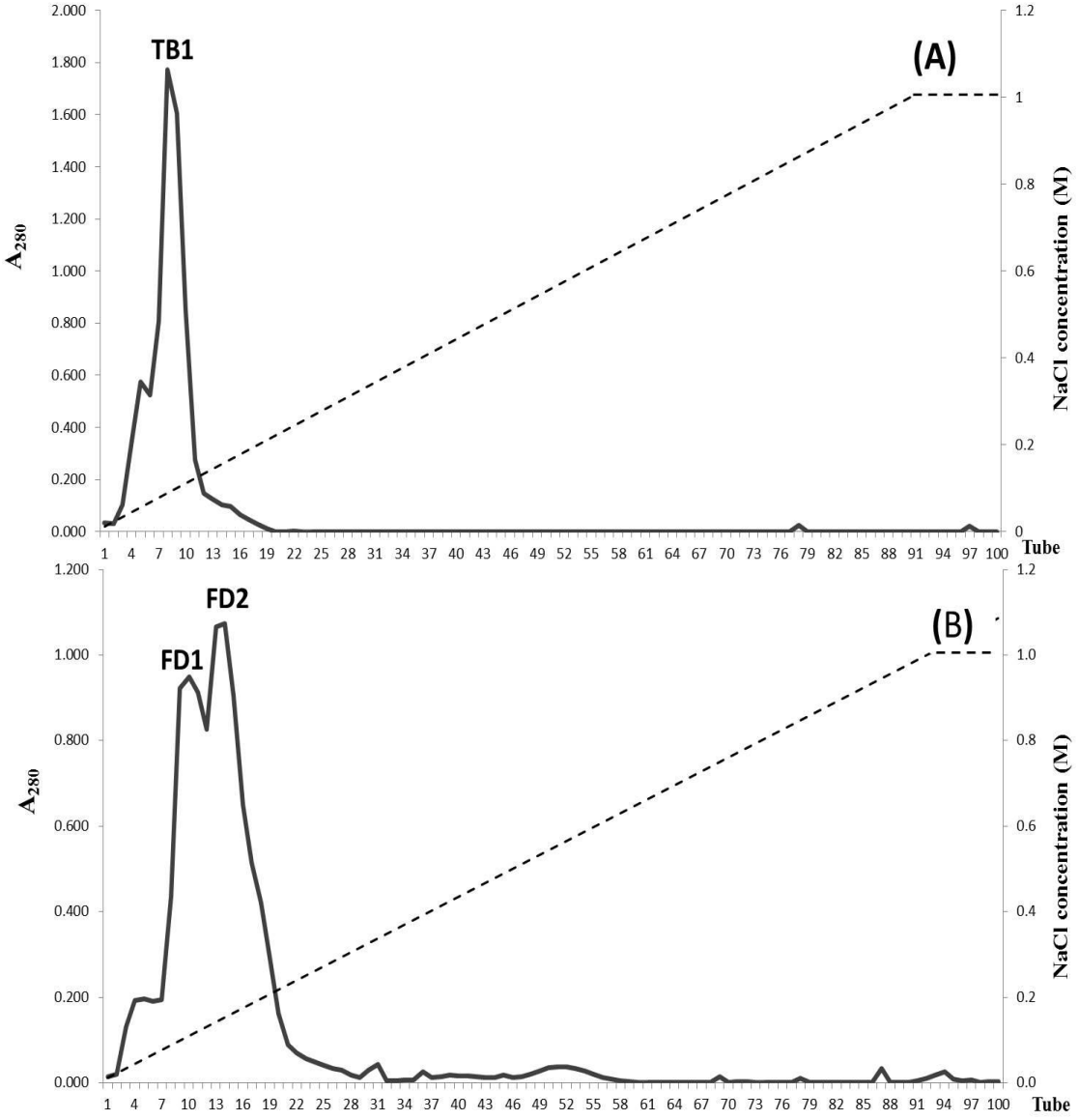

Figure 3.4 SP sephadex® C-25 ion exchange chromatogram eluted with 20 mM sodium acetate buffer pH4.0 with linear gradient NaCl 0-1.0 M at flow rate of 0.6 mL/min. (A): TB fraction and (B): FD fraction

Table 3.4 Antioxidant and antihypertensive activities of bioactive peptide yielded from SP sephadex® C-25 ion exchange chromatography

Sample	ABTS (mM trolox/mg protein)	ACE inhibition (%)
TB	163.15 ± 0.44^{a}	59.33 ± 9.97^{a}
TB1	$114.05 \pm 0.04^{a,b}$	$50.32 \pm 1.56^{a,b}$
FD	250.05 ± 0.02^{c}	79.53 ± 2.00^{c}
FD1	90.25 ± 0.15^{b}	$41.92 \pm 9.46^{a,b}$
FD2	223.95 ± 0.12^{c}	32.56 ± 6.43^{b}

Different letters represent significant differences (p<0.05).

The results suggested that purification with ion exchange chromatography did not enhance their bioactivities. Even if, the same level of antioxidation and ACE inhibition of TB and TB1 were exhibited but TB1 activity was slightly lower than TB fraction. For FD fraction, FD2 showed the similar level of antioxidant activity compared with FD fraction but FD1 considerably lost antioxidant property. Moreover, antihypertensive property was significantly decreased in both FD1 and FD2 fraction (41.92 ± 9.46 and 32.56 ± 6.43%, respectively) compared to original FD fraction (79.53 ± 2.00%). Table 3.5 summarized the bioactivities of purified hydrolysate. Thus, second purification step with ion exchange column was not necessary since this step did not improve the bioactivities. In fact, ion exchange purification did adversely to both antioxidant and antihypertensive activities. Therefore, according to our finding, TB and FD fraction were selected to identify for their peptide sequence with MALDI-TOF/TOF MS/MS technique.

Table 3.5 The summarized bioactivities of purified hydrolysate

Fraction	Protein content (mg)	ABTS (mM trolox/mg protein)	ACE inhibition (%)
Crude Trypsin	1000.0 ± 0.00	205.80 ± 0.29	56.22 ± 2.19
Gel filtration			
-TA	28.85 ± 2.47	116.15 ± 0.70	28.80 ± 9.11
-TB	389.70 ± 37.90	163.15 ± 0.44	59.33 ± 9.97
-TC	341.8 ± 42.99	186.80 ± 0.38	40.59 ± 5.89
Ion exchange			
-TB	389.70 ± 37.90	163.15 ± 0.44	59.33 ± 9.97
-TB1	160.05 ± 9.97	114.05 ± 0.04	50.32 ± 1.56

Table 3.5 The summarized bioactivities of purified hydrolysate (Continued)

Fraction	Protein content (mg)	ABTS (mM trolox/mg protein)	ACE inhibition (%)
Crude Flavourzyme	1000.0 ± 0.00	235.65 ± 0.34	83.60 ± 0.98
Gel filtration			
-FA	16.65 ± 0.64	280.45 ± 0.61	73.69 ± 6.83
-FB	186.2 ± 6.36	113.95 ± 0.10	82.40 ± 2.72
-FC	197.1 ± 35.78	164.90 ± 0.13	68.28 ± 1.26
-FD	377.05 ± 43.77	250.05 ± 0.02	79.53 ± 2.00
Ion exchange			
-FD	377.05 ± 43.77	250.05 ± 0.02	79.53 ± 2.00
-FD1	176.45 ± 34.58	90.25 ± 0.15	41.92 ± 9.46
-FD2	71.7 ± 8.06	266.95 ± 0.12	32.56 ± 6.43

3.4 Peptide Sequencing with MALDI-TOF/TOF

Peptide sequences of TB and FD fractions were identified by MALDI-TOF/TOF mass spectrometer. The MS/MS spectra result was analysed by matching obtained sequence with Ludwig NR Database to identify protein of interest. The MS/MS spectra of TB and FD fractions were presented in Figure 3.5A and 3.5B, respectively. For TB fraction, there were peptides present that did not match to the database. Nevertheless, there were two spectra corresponding with the collagen peptides from *Oreochromis niloticus* in the database. These two spectra consisted of 9- and 18-amino acids and their sequences were GPEGPAGAR (from now on 'peptide 1', MW 810.87 Da) and

GETGPAGPAGAAGPAGPR (from now on ‘peptide 2’, MW 1490.61 Da), respectively. On the contrary, for FD fraction, there were only a few peaks present in the sample and those peaks did not significantly match with any peptide in the database. So, peptide 1 and peptide 2 were subsequently analyzed with *in silico* molecular docking method to evaluate the interaction between amino acid sequence of identified peptide and the ACE active site.

3.5 Evaluation of Identified Peptide Interaction on ACE Active Site

The SYBYL X Molecular Modeling Software was applied for construction of peptide 1 and peptide 2 molecular structures with energy minimized and the structure of peptide 1 and peptide 2 was docked onto the rigid active site of ACE. In order to further evaluate the possibility of distinguishing between the binding modes of peptide 1 and peptide 2 bound onto ACE, molecular docking was performed on an X-ray complex structure of the target enzyme that has been co-crystalized with an K-26 (PDB 4BZR) inhibitor, which had been reported by Kramer et al. (2014). Efficiency of the docking protocol was initially validated by re-docking the K-26 inhibitor onto the apo-enzyme (previously created by a manual removal of the co-crystalized K-26 ligand). The best docked pose, judged by the highest binding affinity ranking, was then superimposed onto the original complex crystal structure. The root-mean-square deviation (RMSD) of the ligand atomic positions was found to be 1.71 Å, which is well within the range of the resolution of the original complex crystal structure (1.84 Å), indicating that the docking protocol is reliable. Some discrepancies between the original ligand atomic positions and those of the re-docked ligand could potentially stem from the flexible nature of the ligand structure that contains several C-C single bonds (Figure 3.6).

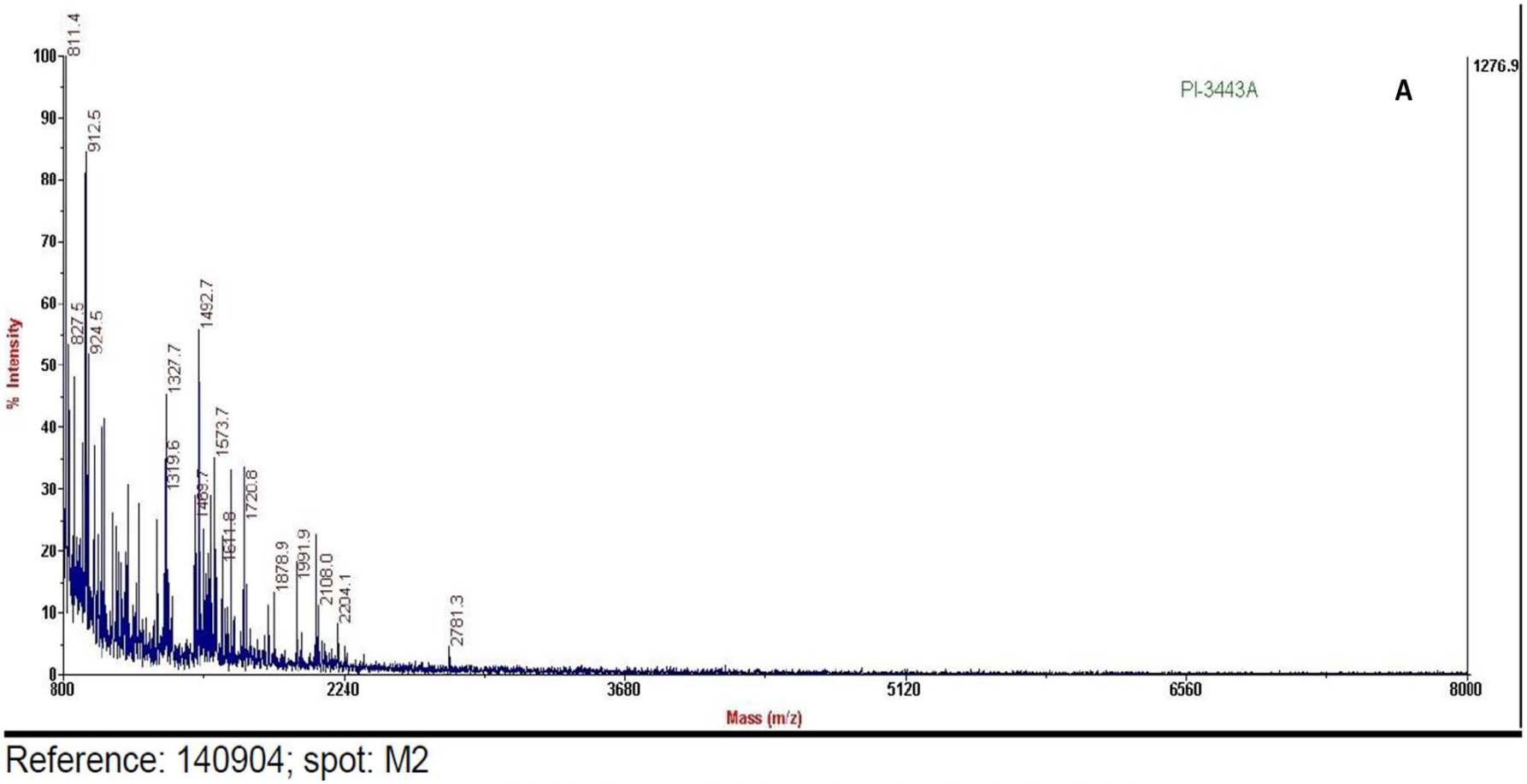

Reference: 140904; spot: M2

Figure 3.5A MS spectra of TB fraction. Two peaks, 811.4 and 1492.7, were significantly matched with the collagen peptide from *Oreochromis niloticus*.

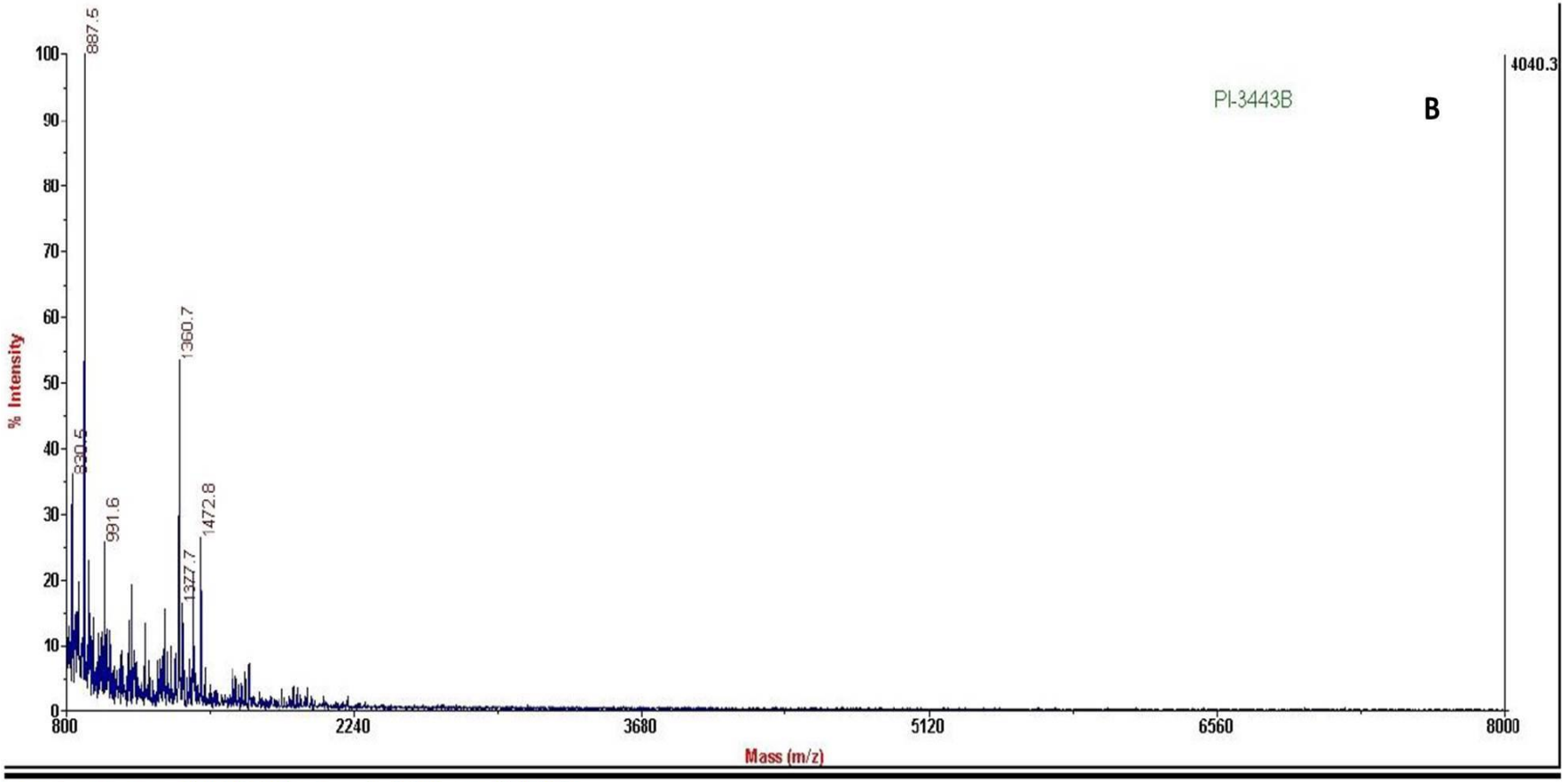

Figure 3.5B MS spectra of FD fraction. A few peaks showed from this fraction and there had no significant matching peptide in the NR Ludwig Database.

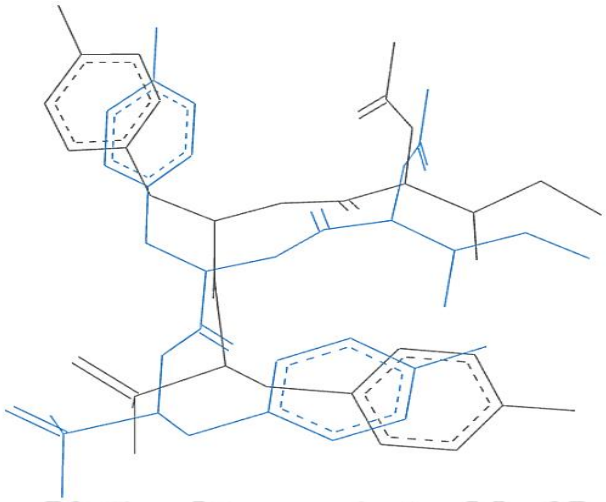

Figure 3.6 Comparison of atomic positions between the original co-crystalized K-26 (blue line) and those of the re-docked K-26 (black line). The RMSD between the two ligand atomic positions was 1.71 Å.

The molecular interactions, including hydrogen bond, electrostatic and hydrophobic interactions, found between the ligands and the active site of ACE were evaluated in comparison with those of K-26 inhibitor. The specific interactions were summarized in Table 3.6. Figure 3.7 displayed the docking poses of ligands (peptide 1, peptide 2 and K-26) onto the active site of ACE. The enzyme pocket of apo-enzyme was shown in Figure 3.7A. Among the 40 conformations, the lowest binding affinity of K-26 inhibitor pose from molecular docking onto the active site of the enzyme was -8.2 kcal/mol (Table 3.6).

Table 3.6 Intermolecular interactions of the docked complexes between peptide 1, peptide 2 or the inhibitor K-26 with the active site residues of ACE.

Compounds	Binding affinity (kcal/mol)	Protein-ligand interactions		
		Hydrogen bond	Electrostatic	Hydrophobic
K-26	-8.2	ALA356:**OC** ALA356:**NH** *ASP358:**OC*** GLU384:**OPO** *TYR523:**OPO***	*Zn^{2+}:**OPO***	TRP357:pi-sigma *HIS387:pi-pi* HIS410:pi-pi VAL518:pi-sigma
Peptide1	- 9.5	GLN281:**OC(Glu3)** GLU411:**OH(Gly4)** *TYR523:**OH***(Gly4) ALA356:**NH**(Gly7) TYR360:**OC(Gly7)** GLU403:**NH(Arg9)** GLY404:**NH(Arg9)**	GLU376:$\mathbf{N^+}$**(Gly1)** ASP453:$\mathbf{N^+}$**(Pro2)** GLU411:$\mathbf{N^+}$**(Pro5)** GLU403:$\mathbf{N^+}$**(Arg9)** ARG522:$\mathbf{O^-}$**(Arg9)** *Zn^{2+}:**OH***(Gly4)	HIS383:pi-sigma**(Pro2)** *HIS387:pi-sigma***(Pro5)** PHE570:pi-sigma**(Arg9)**
Peptide2	-9.3	GLU162:**NH(Gly1)** ASP377:**NH(Gly1)** CYS370:**NH(Gly1)** ALA354:**OC(Gly1)** LYS511:**OC(Glu2)** THR282:**OH(Thr3)** HIS353:**NH(Gly7)** ASN66:**NH(Ala11)** ARG124:**OC(Ala12)** TYR360:**NH(Ala15)** TYR394:**NH(Arg18)** *ASP358:**NH***(Arg18) TYR360:**NH(Arg18)**	GLU162:$\mathbf{N^+}$**(Gly1)** ASP377:$\mathbf{N^+}$**(Gly1)** LYS511:$\mathbf{O^-}$**(Glu2)** ASP358:$\mathbf{N^+}$**(Arg18)** *Zn^{2+}:**OC***(Ala6)	HIS383:pi-sigma**(Pro5)** HIS410:pi-cation**(Arg18)**

Ligand atoms are highlighted in bold letters. Similar interactions among the ligands of the common ACE residues are highlighted in the same font style. Binding affinity of each complex calculated by the docking protocol is also indicated. OC = carbonyl, NH = amine/amide, OPO = phosphate, N+ = nitrogen positive charge, O- = oxygen negative charge.

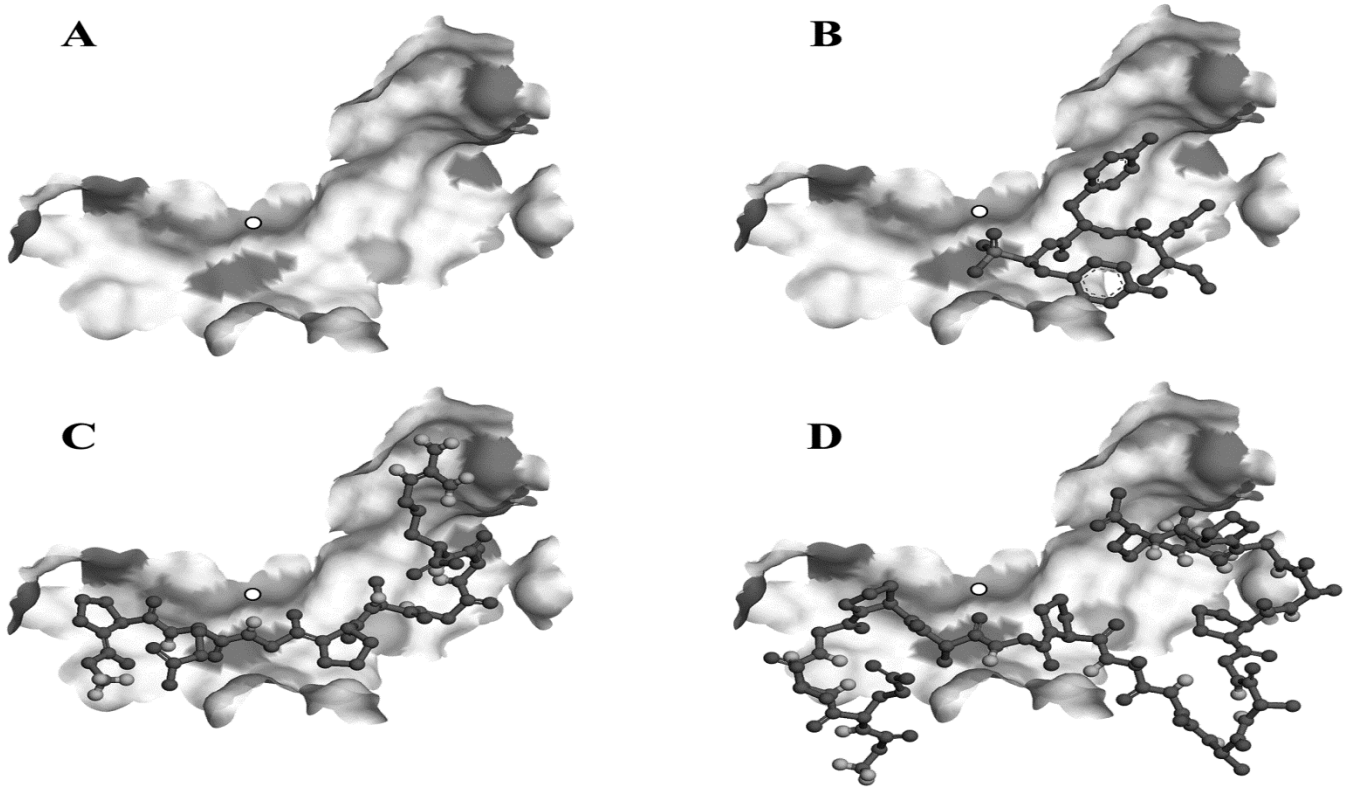

Figure 3.7 Docking poses of ligands onto the active site of ACE. (A) Apo-enzyme generated by a manual removal of original (K-26) ligand from the co-crystal complex structure is shown in a surface model where ionic residues are highlighted in gray patches. A small white circle indicates the location of Zn^{2+} co-factor of the enzyme. (B) K-26 molecule re-docked onto the active site of the enzyme is shown in a ball-and-stick model. Peptide 1 (C) or peptide 2 (D) were also docked into the active site of the same apo-enzyme structure. Light gray atoms are oxygen.

The particular intermolecular interactions between the K-26 ligand and the enzyme pocket were revealed (Figure 3.7B). Four amino acid residues of the enzyme formed the hydrogen bonds with K-26 ligand – two bonds between ALA356 and carbonyl and amine groups of the ligand, one bond between ASP358 to a carbonyl group and two bonds between GLU384 and TYR523 with the phosphate group of the ligand. Electrostatic interaction was also found between the Zn^{2+} co-factor of the enzyme and the phosphate group of the ligand. For hydrophobic interaction, pi-sigma interactions were found at TRP357 and VAL518 residues, and pi-pi interactions were noticed at HIS387 and HIS410 residues.

Figure 3.7C revealed the best conformation of peptide 1 docked onto the active site of ACE, which had better binding affinity (-9.5 kcal/mol) than the case of K-26. For peptide 2, the best pose that docked onto the active site of ACE (Figure 3.7D) gave the similar level of binding affinity (-9.3 kcal/mol). In terms of fitting into the binding pocket of ACE, the docking results suggested that peptide 1 is slightly more superior to peptide 2, although having a similar level of binding affinity. It could imply that the ACE-peptide 1 and ACE-peptide 2 complexes are more stable than the ACE-K-26 complex. Peptide 1 may be a better ligand for the ACE active site cleft than peptide 2.

To validate the results of these two peptides on the antihypertensive activity, peptide 1 and peptide 2 were synthesized by China Peptides Co Ltd. (Shanghai, China) and were used as an inhibitor sample at 1.0 mg/mL concentration. Interestingly, the results exhibited that higher ACE inhibition were noticed in synthesized peptide 2 with 40.52 ± 0.01%. This was slightly higher than that of the synthesized peptide 1, which could inhibit the ACE function with 37.36 ± 0.00%. However, the antihypertensive activity between these two synthesized peptides was not significantly different.